
Conformational flexibility and absolute stereochemistry of (3*R*)-3-hydroxy-4-aryl-*β*-lactams investigated by chiroptical properties and TD-DFT calculations

Daniele Tedesco[1], Riccardo Zanasi[2], Andrea Guerrini[3], Carlo Bertucci[1,*]

[1] *Department of Pharmaceutical Sciences, University of Bologna, Italy;*

[2] *Department of Chemistry and Biology, University of Salerno, Italy;*

[3] *Institute for Organic Synthesis and Photoreactivity (ISOF), National Research Centre (CNR), Bologna, Italy.*

* Corresponding author. E-mail: carlo.bertucci@unibo.it

ABSTRACT

The effect of conformational flexibility on the chiroptical properties of a series of synthetic (3*R*)-3-hydroxy-4-aryl-*β*-lactams of known stereochemistry (**1**-**6**) was investigated by means of electronic circular dichroism (ECD) measurements and time-dependent density functional theory (TD-DFT) calculations. The application of the *β*-lactam sector rules allowed a correct stereochemical characterisation of these compounds, with the exception of a thienyl-substituted derivative (*cis*-**6**). TD-DFT calculations yielded accurate predictions of experimental ECD spectra and $[\alpha]_D$ values, allowing to assign the correct absolute configuration to all the investigated compounds. A detailed analysis of the *β*-lactam ring equilibrium geometry on optimised conformers identified regular patterns for the arrangement of atoms around the amide chromophore, confirming the validity of the *β*-lactam sector rules. However, relevant variations in theoretical chiroptical properties were found for compounds bearing a heterocyclic substituent at C4 or a phenyl substituent at C3, whose conformers deviate from these regular geometric patterns; this behaviour explains the failure of the *β*-lactam sector rules for *cis*-**6**. This study showed the importance of conformational flexibility for the determination of chiroptical properties, and highlighted strengths and weaknesses of the different methods for the stereochemical characterisation of chiral molecules in solution.

KEYWORDS

β-lactams; absolute configuration; conformational flexibility; molecular geometry; *β*-lactam sector rules; optical rotation (OR); electronic circular dichroism (ECD); time-dependent density functional theory (TD-DFT).

INTRODUCTION

β-Lactam rings play a fundamental role in medicinal chemistry: *β*-lactam derivatives have been widely used in therapy as antibiotics, [1-6] cholesterol absorption inhibitors, [7-9] and prostate-specific antigen inhibitors; [10] moreover, their employment as precursors for the asymmetric synthesis of a variety of compounds of medicinal interest, such as proteinogenic and non-proteinogenic amino acids for peptides and peptidomimetics, taxanes, statines and norstatines, is well documented in literature under the name of *β*-lactam synthon method. [11-15] A series of (3*R*)-3-hydroxy-4-aryl-*β*-lactam derivatives (Figures 1-2) was previously synthesised for this purpose [16-19] through the synthetic method of self-regeneration of stereocenters (SRS), [20] consisting in addition reactions of arylimines to lithium enolates of (2*S*,5*S*)-dioxolan-4-ones, which allowed full control of stereochemistry at C3.

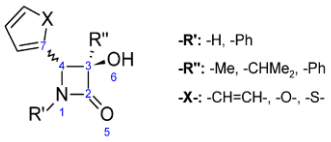

Figure 1. General structure of (3*R*)-3-hydroxy-4-aryl-*β*-lactams.

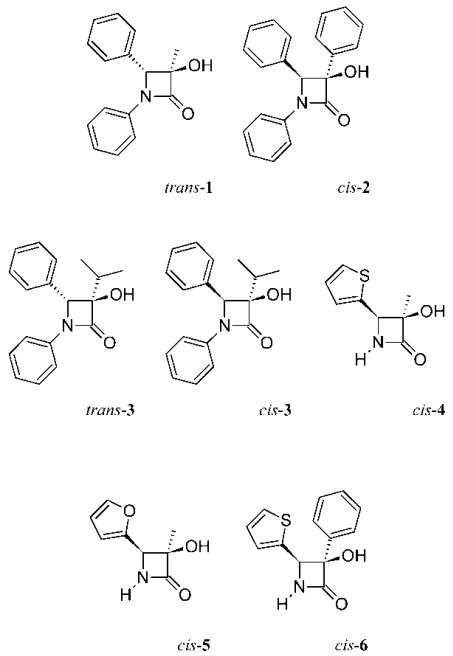

Figure 2. Selected (3*R*)-3-hydroxy-4-aryl-*β*-lactam derivatives.

Stereochemical characterisation is therefore crucial for the employment of these *β*-lactam derivatives as chiral intermediates: for these derivatives, it is mainly concerned with the confirmation of the absolute configuration at C3 and the determination of the relative configuration at C3 and C4, which allows the overall absolute stereochemistry to be consequently deduced. Several methods have been developed and applied to relate the chiroptical properties of *β*-lactams to their stereochemistry. *β*-Lactam sector rules are semi-empirical methods for predicting the Cotton effect (CE) arising from the amide chromophore of the lactam ring, based on the spatial disposition of atoms around the carbonyl group; [21-24] these methods are closely related to the octant rule for the carbonyl chromophore of ketones, [25-27] and proved to be very effective in correlating the absolute configuration of stereogenic atoms around the chromophore to the experimental chiroptical properties, i.e. optical rotation (OR) and electronic circular dichroism (ECD). A semi-empirical helicity rule was proposed, suggesting a strong contribution of the intrinsic chirality of non-planar *β*-lactam rings to the CE of the amide moiety: [28] this method was successfully used to characterise the stereochemistry of small chiral *β*-lactam derivatives. [29] Another helicity rule was proposed for bicyclic *β*-lactam derivatives, relating the CE for the amide chromophore to the absolute stereochemistry at the ring junction carbon atom: [30] the effect of conformational flexibility on the chiroptical properties of these derivatives was also investigated by means of molecular dynamics (MD) and quantum mechanical (QM) calculations. [31] Moreover, the absolute configuration of a different series of 4-substituted (3*R*)-3-hydroxy-*β*-lactam derivatives was reliably determined by application of the exciton-coupled-based zinc-porphyrin tweezer methodology [32,33] combined with molecular mechanical (MM) and QM calculations. [34,35]

Applying the *β*-lactam sector rules to the series of (3*R*)-3-hydroxy-4-aryl-*β*-lactam derivatives under investigation, the signs of the specific rotatory power at the sodium D line ($[\alpha]_D$) and the lowest-energy band of ECD spectra reflect the relative configuration of substituents at C3 and C4: since the substituents at C3 lie on sectors having opposite contributions to the chiroptical properties, the most important contribution is ultimately due to the configuration of the aryl-substituted C4. In

the specific case of (3*R*)-diastereomers, the hydroxyl group at C3 lies on a negative sector and the hydrocarbon substituent at C3 lies on a positive sector; compounds having the aryl substituent at C4 on the same side of the hydroxyl group at C3 (*cis* configuration), therefore lying on a positive sector, are expected to show positive signs of chiroptical properties, while compounds having opposite (*trans*) configuration should show negative signs, since the aryl substituent at C4 lies on a negative sector. A full stereochemical characterisation by means of X-ray crystallography, ECD and nuclear magnetic resonance (NMR) spectroscopies showed that the *β*-lactam sector rules successfully predicted the correct relative and absolute stereochemistry for the series. [36] Nevertheless, these semi-empirical methods failed to predict the correct signs of chiroptical properties for a 4-(thien-2-yl)-substituted derivative (compound *cis*-**6** in Figure 2), whose relative stereochemistry was determined by nuclear Overhauser effect (NOE) and heteronuclear single quantum coherence (HSQC) spectroscopies. [19]

In the present study, the effects of geometric perturbations induced by conformational flexibility on the chiroptical properties of the *β*-lactam ring will be investigated, in order to clarify the reasons behind the failure of *β*-lactam sector rules for the stereochemical characterisation of *cis*-**6** and to have a better insight on the close relationship between molecular geometry and optical activity for this class of molecules. The theoretical chiroptical properties of some selected (3*R*)-3-hydroxy-4-aryl-*β*-lactam derivatives were determined by full QM calculations using time-dependent density functional theory (TD-DFT) [37] and compared to experimental data; the effect of conformational flexibility was subsequently investigated by analysing the variation of theoretical properties as a function of the geometric parameters of the *β*-lactam ring on the QM optimised conformers, as obtained by density functional theory (DFT) [38,39] conformational analysis.

EXPERIMENTAL

Materials

Experimental measurements and QM calculations were performed on the following (3*R*)-3-hydroxy-4-aryl-*β*-lactam derivatives (Figure 2): (3*R*,4*R*)-3-hydroxy-3-methyl-1,4-diphenylazetidin-2-one (*trans*-**1**; $C_{16}H_{15}NO_2$, MW: 253.30), (3*R*,4*S*)-3-hydroxy-1,3,4-triphenylazetidin-2-one (*cis*-**2**; $C_{21}H_{17}NO_2$, MW: 315.17), (3*R*,4*R*)-3-hydroxy-1,4-diphenyl-3-(propan-2-yl)azetidin-2-one (*trans*-**3**; $C_{18}H_{19}NO_2$, MW: 281.35) and its (3*R*,4*S*)-diastereomer (*cis*-**3**), (3*R*,4*R*)-3-hydroxy-3-methyl-4-(thiophen-2-yl)azetidin-2-one (*cis*-**4**; $C_8H_9NO_2S$, MW: 183.23), (3*R*,4*S*)-4-(furan-2-yl)-3-hydroxy-3-methylazetidin-2-one (*cis*-**5**; $C_8H_9NO_3$, MW: 167.16), and (3*R*,4*R*)-3-hydroxy-3-phenyl-4-(thiophen-2-yl)azetidin-2-one (*cis*-**6**; $C_{13}H_{11}NO_2S$, MW: 245.30). These derivatives were synthesised according to reported procedures; experimental $[\alpha]_D$ values were also already reported and are summarised in Table 1. [16-19,36]

Table 1. Experimental and calculated values of specific rotatory power at the sodium D line (589.3 nm) for the series of selected (3*R*)-3-hydroxy-4-aryl-*β*-lactam derivatives **1**-**6**.

	trans-**1**	*cis*-**2**	*trans*-**3**	*cis*-**3**	*cis*-**4**	*cis*-**5**	*cis*-**6**
experimental $[\alpha]_D$ (deg)	−134.0 [b]	+52.6 [b]	−64 [c]	+180 [c]	+70 [c]	+70 [c]	−71 [d]
solvent	chloroform	chloroform	chloroform	chloroform	acetone	acetone	chloroform
calculated $[\alpha]_D$ (deg) [a]							
ΔE_{QM} *-based average*	−104.9	+111.2	−27	+147	+14	−29	−70
(difference with exp.)	(+29.1)	(+58.6)	(+37)	(−33)	(−56)	(−99)	(+1)
ΔG *-based average*	−105.9	+106.9	−25	+150	+14	−1	−102
(difference with exp.)	(+28.1)	(+54.3)	(+39)	(−30)	(−56)	(−71)	(−31)
conformers	2	5	4	9	6	5	7
SSM, ΔE_{QM} *-based average*					+69	+106	
(difference with exp.)					(−1)	(+36)	
SSM, ΔG *-based average*					+88	+180	
(difference with exp.)					(+18)	(+110)	
conformers					7	6	

[a] Calculated using Boltzmann statistics at 298.15 K. [b] Measured at 19 °C (292.15 K). [16] [c] Measured at 22 °C (295.15 K). [17] [d] Measured at 20 °C (293.15 K). [19]

UV and ECD spectra of *trans*-**1** (concentration: 0.4 mM; pathlength: 0.1 cm; range: 350–200 nm), *trans*-**3** (3.5 mM; 0.01 cm; 350–200 nm), *cis*-**3** (3.5 mM; 0.01 cm; 350–220 nm) and *cis*-**4** (5.5 mM;

0.01 cm; 300–190 nm) were recorded in 2-propanol (Sigma-Aldrich, Milan, Italy) on a Jasco (Tōkyō, Japan) J-720 spectropolarimeter at room temperature. UV and ECD spectra of *cis*-**6** (1.0 mM; 0.1 cm; 350–220 nm) were recorded in 2-propanol (Sigma-Aldrich, Milan, Italy) on a Jasco (Tōkyō, Japan) J-810 spectropolarimeter at room temperature.

MM conformational search

A preliminary conformational analysis on all the *β*-lactam derivatives under examination was carried out through MM calculations using the Spartan'02 software package. [40] Conformational search was performed using the systematic algorithm and conformer distribution was determined at the MMFF94s [41] level. Conformers having relative energies (ΔE_{MM}) within a threshold value of 5 kcal mol^{-1} were considered for geometry optimisation at the QM level.

DFT geometry optimisation

DFT geometry optimisation calculations were carried out using B97D, a generalised gradient approximation (GGA) functional with semi-empirical corrections for dispersion, [42,43] as implemented in the Gaussian 09 software package. [44] A triple-ζ double polarisation (TZ2P) basis set of Gaussian-type orbitals (GTOs) was employed in the calculations. For hydrogen and first-row atoms, the basis set consisted in Dunning's [5*s*3*p*/3*s*] contraction [45] of Huzinaga's primitive [10*s*6*p*/5*s*] set [46] with 2 sets of polarisation functions (α_p = 1.5, 0.375 for H; α_d = 1.5, 0.375 for C; α_d = 1.6, 0.4 for N; α_d = 1.7, 0.425 for O); for sulphur, McLean and Chandler's [6*s*5*p*] contraction [47] of Huzinaga's primitive [12*s*9*p*] set [48] with 2 sets of polarisation functions (α_d = 1.4, 0.35) was used. Long-range solvent effects were taken into account by using the polarisable continuum model in its integral equation formalism (IEFPCM), [49] as implemented in the Gaussian 09 software package. The suitable solvation model was chosen depending on the environment of experimental data: chloroform for OR calculations on *trans*-**1**, *cis*-**2**, *trans*-**3**, *cis*-**3** and *cis*-**6**, acetone for OR calculations on *cis*-**4** and *cis*-**5**, 2-propanol for ECD calculations on *trans*-

1, *trans*-**3**, *cis*-**3**, *cis*-**4** and *cis*-**6**. Conformational clustering was performed for optimised geometries having root mean square distances (RMSD) below 0.01 Å for heavy atoms, as obtained after alignment of the azetidinone skeleton; geometry alignment and RMSD determination were carried out using the VMD molecular graphics software. [50] The Boltzmann distribution of conformers in a given solvent, at 298.15 K and 1 atm, was subsequently calculated for each compound on the basis of the relative electronic energies (ΔE_{QM}) and relative free energies (ΔG).

Solvated supermolecule (SSM) approach

A method of explicit treatment of solvent molecules around a solute in QM calculations, referred to in literature as the solvated supermolecule (SSM) approach, [49] was employed for the determination of solvent-induced conformational flexibility and its effect on the chiroptical properties of *β*-lactam derivatives. SSM calculations were carried out on *cis*-**4** and *cis*-**5** following the same protocol used for standard calculations: MM conformational search was performed on solute-solvent clusters (labelled *cis*-**4*** and *cis*-**5***, respectively) obtained by placing a molecule of acetone close to each of the 2 H-bond donor groups (the lactam NH group and the hydroxyl group at C3) and with the carbonyl group oriented to interact through hydrogen bonding (Figure 3).

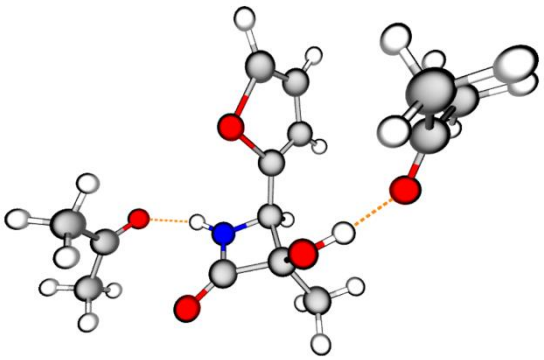

Figure 3. Input geometry for the MM conformational search on *cis*-**5***.

Conformations having $\Delta E_{MM} \leq 5$ kcal mol^{-1} were considered for DFT geometry optimisation. An early optimisation step using the B97D functional and the 6-31G* basis set [51-55] was introduced for *cis*-**5*** in order to reduce the time of analysis, since the 6-31G* basis set is less expensive than

TZ2P in terms of computational time: B97D/6-31G* conformers having $\Delta E_{QM} \leq 2.5$ kcal mol^{-1} were subsequently optimised at the B97D/TZ2P level. On the other hand, MM conformers of *cis*-**4*** were directly optimised at the B97D/TZ2P level. The IEFPCM solvation model for acetone was employed in DFT calculations in order to account for bulk effects.

TD-DFT calculations of chiroptical properties

The determination of theoretical chiroptical properties [56] was carried out by means of TD-DFT calculations using the Gaussian 09 software package. [44] Calculations were performed on the B97D/TZ2P optimised geometries of compounds **1**-**6** and on the solute-solvent clusters *cis*-**4*** and *cis*-**5***, employing the PBE0 exchange-correlation functional [57-59] and the TZ2P basis set.

Theoretical $[\alpha]_D$ values, as well as excitation wave numbers (σ_{mn}) and rotational strengths (R_{mn}) for the lowest 50 excited states, were calculated on each optimised conformer using the same IEFPCM solvation model employed in the optimisation process. Theoretical ECD spectra as a function of wave number, $\Delta\varepsilon_{calc}(\sigma)$, were derived for each conformer by approximation of R_{mn} values to Gaussian functions and summation over all excited states; [60] in this study, the half-bandwidth of Gaussian functions ($\Delta\sigma$) was set to 0.4 eV. Conformational averaging, based on the Boltzmann distribution of conformers, was subsequently performed to obtain the theoretical properties of the β-lactam derivatives at equilibrium; [56] calculated ECD spectra were then converted in wavelength scale for a convenient comparison with experimental data.

RESULTS AND DISCUSSION

Structure and geometric features of β-lactam derivatives

The (3*R*)-3-hydroxy-4-aryl-β-lactams under investigation show the following structural patterns (Figure 1): **a)** the aromatic substituent at C4 is either a phenyl ring (X = −CH=CH− for *trans*-**1**, *cis*-**2**, *trans*-**3** and *cis*-**3**) or a five-membered heterocycle (X = −S− for *cis*-**4** and *cis*-**6**; X = −O− for *cis*-**5**); **b)** non-heteroaromatic derivatives are all phenyl-substituted at N1 (R′ = −Ph), while heteroaromatic derivatives are unsubstituted (R′ = −H); **c)** the hydrocarbon substituent at C3 may be either aliphatic (R″ = −Me, $-CHMe_2$) or aromatic (R″ = −Ph).

The four-membered *β*-lactam ring is a non-planar structure subject to a significant angle strain, which causes the geometry of the amide chromophore to deviate from planarity. [29] The conformational strain of the *β*-lactam ring may be conveniently characterised by a set of 4 dihedral angles: ψ_1 (O5−C2−N1−R′1) describes the torsion and intrinsic chirality of the amide C−N bond, ψ_2 (O5−C3−N1−C2) and ψ_3 (R′1−C2−C4−N1) describe the pyramidalisation of C2 and N1, respectively, and ψ_4 (O5−C2−N1−C4) describes the deviation of C4 from the hypothetical plane of the carbonyl group (O5−C2−N1 plane). Additional conformational flexibility arises from the orientation of substituents at C3 and C4: ϕ_1 (C3−C4−C7−X) describes the orientation of the aromatic substituent at C4 (X = C for phenyl, O for furyl, S for thienyl), ϕ_2 (C4−C3−R″1−R″2) describes the orientation of hydrocarbon substituents other than methyl groups at C3 (R″2 = H for isopropyl, C for phenyl), and ω (C4−C3−O6−H6) describes the orientation of the O−H bond for the hydroxyl group at C3.

MM conformational search

Relative energies and fractional populations for the MM conformers of *cis*-**6** are reported in Table 2; full details on the geometric parameters, energies and fractional populations for the MM conformers of all the *β*-lactam derivatives are given in the Supplementary Information (Tables S1-S9).

Table 2. Relative energies and fractional equilibrium populations for the conformers of *cis*-**6**, as obtained after MM conformational search.

Conformer	ΔE_{MM} (kcal mol^{-1})	χ_{MM} [a]
cis-**6a**	0.000	0.6596
cis-**6b**	0.878	0.1497
cis-**6c**	1.438	0.0582
cis-**6d**	1.493	0.0530
cis-**6e**	1.584	0.0455
cis-**6f**	1.801	0.0315
cis-**6g**	3.528	0.0017
cis-**6h**	4.038	0.0007

[a] Calculated using Boltzmann statistics at 298.15 K.

As a result, two conformers for *trans*-**1** (labelled *trans*-**1a**–**b**), eight for *cis*-**2** (*cis*-**2a**–**h**), four for *trans*-**3** (*trans*-**3a**–**d**), nine for *cis*-**3** (*cis*-**3a**–**i**), six for *cis*-**4** (*cis*-**4a**–**f**), eight for *cis*-**4*** (*cis*-**4*a**–**h**), six for *cis*-**5** (*cis*-**5a**–**f**), twenty-three for *cis*-**5*** (*cis*-**5*a**–**w**) and eight for *cis*-**6** (*cis*-**6a**–**h**) were found below the energy threshold value of 5 kcal mol^{-1} and were optimised at the DFT level.

DFT geometry optimisation

Relative electronic and free energies, and corresponding fractional populations for the DFT conformers of *cis*-**6** are reported in Table 3. Full details on geometric parameters, energies and fractional populations for the DFT conformers of all the *β*-lactam derivatives, as well as graphical representations of the most populated conformers, are given in the Supplementary Information (Tables S10-S19; Figures S1-S9).

The preliminary B97D/6-31G* optimisation step for *cis*-**5*** identified sixteen SSM conformations having $\Delta E_{QM} \leq 2.5$ kcal mol^{-1}. After RMSD analysis, some optimised geometries were clustered: *cis*-**2b/f**, *cis*-**2c/d/e**, *cis*-**5e/f**, *cis*-**5*l/p**, *cis*-**5*r/u**, *cis*-**5*b/v**, *cis*-**5*c/q**, *cis*-**5*m/o** and *cis*-**6e/f**. The B97D/TZ2P optimisation step reduced the number of SSM conformations to seven for *cis*-**4*** and six for cis-**5***, since the interaction between acetone and hydrogen-bond donor groups was lost during the optimisation process for some conformers.

Table 3. Relative energies and fractional equilibrium populations for the conformers of *cis*-**6**, as obtained after DFT geometry optimisation (B97D/TZ2P) in chloroform and 2-propanol (IEFPCM solvation models).

Solvent	Conformer	ΔE_{QM} (kcal mol^{-1})	χ_{QM} [a]	ΔG (kcal mol^{-1})	χ_{G} [a]
Chloroform	*cis*-**6c**	0.000	0.5616	0.000	0.4583
	cis-**6f**	0.492	0.2448	0.390	0.2374
	cis-**6e**	0.492	— [b]	0.351	— [b]
	cis-**6g**	1.487	0.0456	1.099	0.0716
	cis-**6h**	1.527	0.0427	1.092	0.0725
	cis-**6b**	1.534	0.0421	1.209	0.0595
	cis-**6d**	1.698	0.0319	1.279	0.0529
	cis-**6a**	1.713	0.0311	1.340	0.0478
2-Propanol	*cis*-**6c**	0.000	0.6271	0.000	0.3427
	cis-**6e**	0.679	0.1994	0.136	0.2726
	cis-**6f**	0.679	— [b]	0.137	— [b]
	cis-**6g**	1.429	0.0562	0.919	0.0727
	cis-**6h**	1.649	0.0388	0.299	0.2068
	cis-**6b**	1.797	0.0302	1.260	0.0409
	cis-**6d**	1.909	0.0250	1.293	0.0387
	cis-**6a**	1.950	0.0233	1.536	0.0257

[a] Calculated using Boltzmann statistics at 298.15 K. [b] RMSD values for *cis*-**6e**/**f**: 0.0050 Å (chloroform), 0.0004 Å (2-propanol).

Experimental and TD-DFT theoretical chiroptical properties

The comparison between conformationally averaged OR calculations and experimental data is shown in Table 1, while the comparison between experimental and theoretical ECD data for *trans*-**1**, *trans*-**3**, *cis*-**3**, *cis*-**4** and *cis*-**6** are reported in Table 4 and Figure 4.

Table 4. Experimental and calculated data for the ECD bands of *trans*-**1**, *trans*-**3**, *cis*-**3**, *cis*-**4** and *cis*-**6** in the 350−200 nm range.

	trans-**1**	*trans*-**3**	*cis*-**3**	*cis*-**4**	*cis*-**6**
experimental $\Delta\varepsilon_{max}$, M^{-1} cm^{-1} (λ_{max}, nm)	−8.4 (246) +2.7 (212)	−13.7 (248)	+10.6 (248)	−1.4 (245) +11.9 (223)	−4.5 (246) +2.0 (219) −4.2 (205)
calculated $\Delta\varepsilon_{max}$, [a] M^{-1} cm^{-1} (λ_{max}, nm)					
ΔE_{QM} *-based average*	−9.6 (251) —	−7.2 (255)	+13.8 (257)	— +12.2 (227)	−5.1 (244) +3.5 (220) −3.2 (206)
ΔG *-based average*	−9.6 (251) —	−7.2 (255)	+14.2 (256)	— +12.5 (228)	−13.2 (246) +5.9 (219) −0.6 (205)
conformers	2	4	9	6	7

[a] Calculated using Boltzmann statistics at 298.15 K.

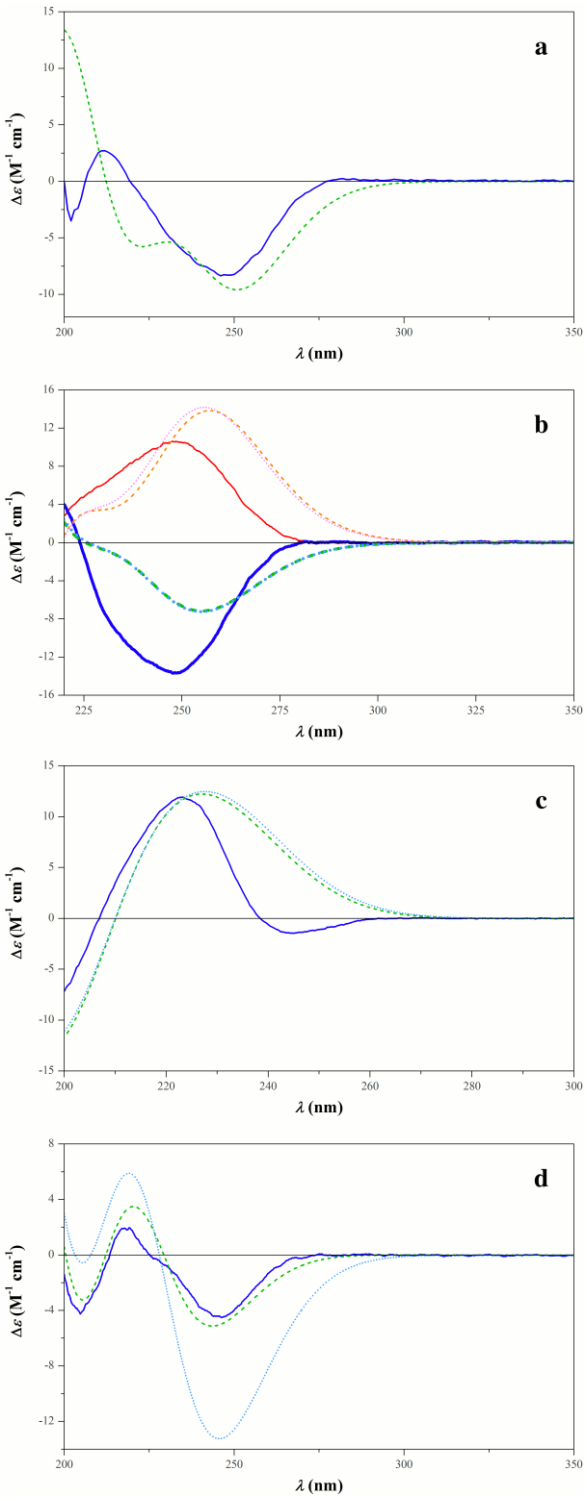

Figure 4. Comparison between experimental and theoretical ECD spectra for selected (3*R*)-3-hydroxy-4-aryl-*β*-lactam derivatives. *Solid*, experimental in 2-propanol. *Dashed*, theoretical (PBE0/TZ2P//B97D/TZ2P, IEFPCM solvation model for 2-propanol), ΔE_{QM}-based averaging, $\Delta\sigma$ = 0.4 eV. *Dotted*, theoretical (PBE0/TZ2P//B97D/TZ2P, IEFPCM solvation model for 2-propanol), ΔG-based averaging, $\Delta\sigma$ = 0.4 eV. **a)** *trans*-**1**; **b)** *cis*-**3** (thin) and *trans*-**3** (bold); **c)** *cis*-**4**; **d)** *cis*-**6**.

Calculated $[\alpha]_{\mathrm{D}}$ values for each optimised conformer are reported in the Supplementary Information (Tables S10-S19), as well as experimental UV and ECD spectra (Figures S10-S13),

calculated R_{mn} values for the first 25 low-energy electronic transitions of each conformer (Tables S20-S23) and Pearson correlation coefficients (r) [61] for the comparison between experimental and theoretical ECD spectra (Table S24).

As a general trend, good agreement between experimental and theoretical properties was found for all the examined compounds, irrespective of the type of relative energies used in the conformational averaging process. While ΔG-based Boltzmann populations are usually preferred in the description of conformationally-averaged chiroptical properties, [56,62] the accuracy of calculated ΔG values is strongly dependent upon the size of the molecular system and other factors limiting the ability to calculate the appropriate entropy terms and enthalpy corrections; ΔE_{QM}-based populations may perform better when errors in the calculation of ΔG values become relevant. [56] In the specific case of TD-DFT calculations on *cis*-**6**, ΔE_{QM}-based conformational averaging yielded better correlation with experimental data, which were reproduced in avery accurate fashion (difference between calculated and experimental $[\alpha]_{\mathrm{D}}$: +1°; r = 0.9264 for ECD comparison; Figure 4d).

TD-DFT calculations using IEFPCM solvation models, without treatment of solvent molecules at a QM level, were sufficient to yield good agreement with experimental data in chloroform and 2-propanol. Poorer correlation with experimental data in acetone was found for *cis*-**4** and *cis*-**5** (differences between ΔE_{QM}-averaged calculations and experimental $[\alpha]_{\mathrm{D}}$ values were −56° and −99°, respectively); for the latter compound, calculated and experimental $[\alpha]_{\mathrm{D}}$ values had opposite sign.

The application of the SSM approach was then limited to OR calculations in acetone for three reasons: **a)** single-wavelength OR calculations are much more sensitive than full-spectrum ECD calculations to systematic errors due to the approximations made in TD-DFT calculations; [56] **b)** the poorer correlation between theoretical and experimental data for OR calculations in acetone with respect to chloroform could suggest a stronger effect of hydrogen bonding on the conformational flexibility; **c)** OR calculations are less expensive than ECD calculations in terms of

computational time. A better description of short-range interactions between solute and solvent, obtained through the SSM approach, improved the accuracy of the calculations (differences between ΔE_{QM}-averaged SSM calculations and experimental $[\alpha]_D$ values were −1° and +34° for *cis*-**4** and *cis*-**5**, respectively).

TD-DFT calculations are therefore able to confirm the stereochemistry of all the *β*-lactam derivatives under investigation, including compound *cis*-**6**, for which the *β*-lactam sector rules were unable to predict the correct absolute configuration at C4.

Conformational flexibility and effect on chiroptical properties

Once the predictive capability of TD-DFT calculations was tested and validated, DFT geometries were thoroughly analysed to explore a possible correlation between the variation of geometric features among different optimised conformations and the variation of theoretical chiroptical properties, i.e. calculated $[\alpha]_D$ values. Tables 5 and 6 list the geometric parameters of all the relevant DFT conformers, sorted by decreasing order of theoretical $[\alpha]_D$ values.

Geometry of the β-lactam ring

Excluding *cis*-**6** and the SSM conformations (*cis*-**4*** and *cis*-**5***), regular patterns in the non-planarity features of the *β*-lactam ring can be identified among optimised conformers with the same relative configuration: all *trans* conformers show positive values for the torsion angle of the amide (ψ_1) and negative values for the pyramidalisation of C2 (ψ_2) and N1 (ψ_3). Conversely, most of the *cis* conformers show the opposite pattern, i.e. negative for ψ_1 and positive for ψ_2 and ψ_3; a notable exception is represented by *cis*-**2**, whose geometric properties will be discussed later. The helicity rule, [29] which predicts a negative contribution to OR for positive torsion angles of the amide (ψ_1) and a positive contribution to OR for negative ψ_1 angles, is also consistent with the regular geometric patterns observed for DFT conformers: positive ψ_1 angles for *trans* conformers and negative ψ_1 angles for *cis* conformers. Moreover, almost all conformers show positive values

for the deviation of C4 from the plane of the carbonyl group (ψ_4), irrespective of the relative configuration.

Table 5. Theoretical values of specific rotatory power (sorted in decreasing order) and geometrical parameters for the conformers of *trans*-**1**, *cis*-**2**, *trans*-**3**, *cis*-**3** and *cis*-**6**, as obtained after DFT geometry optimisation (B97D/TZ2P) and TD-DFT calculation of optical rotation (PBE0/TZ2P) in chloroform (IEFPCM solvation model).

Conformer	χ_{QM} [a]	$[\alpha]_D$ (deg)	ψ_1 (deg)	ψ_2 (deg)	ψ_3 (deg)	ψ_4 (deg)	ϕ_1 (deg)	ϕ_2 (deg)	ω (deg)
trans-**1a**	0.7377	**−90.2**	+2.23	−0.47	−2.39	+176.55	+79.05	—	+173.52
trans-**1b**	0.2623	**−148.5**	+2.12	−0.02	−2.22	+175.99	+78.84	—	−99.56
cis-**2a**	0.0623	**+167.6**	−4.48	−0.28	+1.13	+178.22	+107.48	+87.28	+176.97
cis-**2c**	0.3825	**+165.3**	−4.16	−0.24	+0.16	+175.61	+103.54	+71.06	+38.99
cis-**2b**	0.4214	**+134.3**	−4.42	−0.19	+0.50	+176.18	+102.14	+83.90	+37.55
cis-**2g**	0.0537	**+42.9**	−4.07	+0.09	+1.36	+178.64	+109.40	+46.65	−90.09
cis-**2h**	0.0801	**−266.6**	−2.64	+0.38	+1.05	+178.88	+105.54	+137.43	−68.04
trans-**3a**	0.6954	**−8.9**	+2.04	−0.83	−2.66	+176.32	+71.16	−46.79	+168.79
trans-**3b**	0.0229	**−31.4**	+6.15	−1.06	−4.70	+176.02	+87.96	−176.17	+169.28
trans-**3d**	0.2644	**−63.8**	+1.41	−0.25	−2.42	+175.04	+71.91	−43.81	−95.13
trans-**3c**	0.0173	**−194.5**	+9.11	−1.09	−6.79	+173.68	+105.15	+54.82	+163.31
cis-**3c**	0.0188	**+226.5**	−5.76	+0.17	+1.60	+176.98	+104.53	−175.15	+171.98
cis-**3b**	0.0137	**+205.3**	−5.08	+0.13	+1.28	+176.99	+108.48	−49.33	+168.57
cis-**3h**	0.0389	**+180.7**	−5.10	+0.53	+2.28	+179.12	+106.49	−173.82	−65.61
cis-**3d**	0.5548	**+161.3**	−6.01	+0.23	+1.12	+175.18	+101.66	−175.34	+39.49
cis-**3e**	0.0271	**+144.1**	−3.99	+0.44	+1.92	+179.67	+109.34	−46.43	−72.90
cis-**3a**	0.2497	**+142.1**	−5.11	+0.22	+0.73	+175.05	+102.78	−47.55	+41.69
cis-**3g**	0.0047	**+107.8**	−4.53	+0.16	+0.74	+175.94	+106.89	+66.16	+160.68
cis-**3i**	0.0042	**+67.2**	−3.59	+0.56	+1.45	+178.49	+105.88	+67.45	−77.92
cis-**3f**	0.0883	**+36.7**	−4.72	+0.45	+0.34	+173.82	+103.22	+68.86	+41.22
cis-**6c**	0.5616	**+60.9**	−0.68	−0.13	−1.14	+175.65	+100.45	+83.06	+36.00
cis-**6d**	0.0319	**−6.6**	−4.83	+0.13	+2.14	−179.48	+107.85	+47.32	−90.69
cis-**6a**	0.0311	**−181.9**	+2.78	−0.22	−1.95	+177.58	+102.95	+119.54	+165.46
cis-**6f**	0.2448	**−224.6**	−5.30	−0.10	+1.08	+176.92	−72.60	+72.44	+42.70
cis-**6h**	0.0427	**−284.9**	−7.39	+0.10	+3.84	−177.16	−62.14	+43.26	−87.70
cis-**6g**	0.0456	**−309.4**	+0.05	+0.03	+0.18	−179.85	+106.38	+135.98	−66.32
cis-**6b**	0.0421	**−417.5**	−1.07	−0.24	+0.18	+179.75	−68.59	+108.86	+167.84

[a] Calculated using Boltzmann statistics at 298.15 K, based on relative electronic energies.

Orientation of aromatic substituents at C4

Theoretical OR values for the conformers of non-heteroaromatic derivatives are in agreement to the *β*-lactam sector rules, i.e. *trans* conformers show negative $[\alpha]_D$ values and *cis* conformers show positive $[\alpha]_D$ values. On the other hand, $[\alpha]_D$ values for the conformers of heteroaromatic

derivatives show a strong dependence upon the orientation of the heterocycle (ϕ_1; Figure 5).

Table 6. Theoretical values of specific rotatory power (sorted in decreasing order) and geometrical parameters for the conformers of *cis*-**4**, *cis*-**5**, *cis*-**4*** and *cis*-**5***, as obtained after DFT geometry optimisation (B97D/TZ2P) and TD-DFT calculation of optical rotation (PBE0/TZ2P) in acetone (IEFPCM solvation model).

Conformer	χ_{QM} [a]	$[\alpha]_D$ (deg)	ψ_1 (deg)	ψ_2 (deg)	ψ_3 (deg)	ψ_4 (deg)	ϕ_1 (deg)	ω (deg)
cis-**4a**	0.0054	**+203.4**	−3.38	+0.44	+0.95	+177.78	+98.40	−179.07
cis-**4e**	0.0180	**+185.8**	−5.74	+0.66	+2.53	+179.49	+98.20	−83.36
cis-**4c**	0.5891	**+120.1**	−3.09	+0.53	+0.42	+176.21	+100.92	+39.55
cis-**4d**	0.0083	**−67.9**	−6.39	+0.45	+2.44	+178.88	−70.06	+179.31
cis-**4f**	0.0288	**−136.5**	−8.04	+0.64	+3.69	−179.62	−68.89	−84.03
cis-**4b**	0.3503	**−162.5**	−6.77	+0.60	+2.19	+177.18	−71.77	+44.60
cis-**5c**	0.0065	**+218.8**	−3.36	+0.46	+0.85	+177.43	+95.74	−178.26
cis-**5f**	0.0170	**+179.1**	−5.56	+0.71	+2.16	+178.40	+95.34	−90.02
cis-**5d**	0.5176	**+127.1**	−3.80	+0.50	+0.81	+176.66	+100.70	+39.55
cis-**5b**	0.0067	**−130.4**	−2.48	+0.49	+0.29	+176.63	−62.90	−176.00
cis-**5a**	0.4523	**−217.6**	−4.00	+0.46	+0.79	+176.40	−54.31	+48.29
cis-**4*c**	0.0043	**+251.2**	+0.72	+0.62	−0.32	+178.49	+96.01	+143.37
cis-**4*b**	0.0098	**+139.4**	−14.47	+1.06	+7.31	−177.40	−72.92	+77.88
cis-**4*h**	0.2122	**+119.5**	−0.88	+0.58	−0.20	+176.90	−69.30	−79.92
cis-**4*d**	0.1423	**+117.5**	+5.05	+0.26	−3.02	+175.98	+108.15	−81.68
cis-**4*f**	0.5035	**+56.6**	−5.36	+0.60	+2.14	+179.03	+112.28	−81.76
cis-**4*a**	0.0127	**+34.7**	−0.06	+0.04	−0.81	+177.15	−123.72	+52.40
cis-**4*e**	0.1152	**−39.1**	+1.36	+0.45	−1.53	+175.75	−97.95	+68.61
cis-**5*a**	0.0932	**+313.6**	−1.64	+0.54	+0.36	+177.88	+101.11	−80.12
cis-**5*e**	0.0896	**+222.0**	+0.48	+0.21	−0.15	+179.67	+111.42	−66.71
cis-**5*b**	0.0040	**+211.5**	−0.32	+0.31	−0.04	+178.74	+96.80	+163.33
cis-**5*u**	0.3616	**+156.8**	+3.79	+0.66	−2.59	+174.70	−62.15	−78.96
cis-**5*i**	0.0134	**+4.2**	+9.30	+0.46	−5.23	+173.70	−64.01	+146.43
cis-**5*p**	0.4382	**−2.2**	−8.87	+0.42	+4.40	−177.43	+111.30	−67.08

[a] Calculated using Boltzmann statistics at 298.15 K, based on relative electronic energies.

Figure 5. B97D/TZ2P optimised conformers of *cis*-**5**. Solvation model: acetone (IEFPCM). *Left*, conformers with positive values of ϕ_1 (*cis*-**5c**, *cis*-**5d** and *cis*-**5f**). *Right*, conformers with negative values of ϕ_1 (*cis*-**5a** and *cis*-**5b**). Dihedral angles are reported in Table 6.

Conformers having the heteroatom oriented on the opposite side with respect to the *β*-lactam ring (positive ϕ_1 values) follow the general trend and their OR is correctly predicted by the *β*-lactam sector rules. Conformers having the heteroatom oriented towards the *β*-lactam ring (negative ϕ_1 values) show an opposite trend and the calculated $[\alpha]_D$ values are in discordance with the *β*-lactam sector rules.

*Conformational flexibility of cis-**2***

The geometric features of *cis*-**2** deserve a deeper analysis: this derivative bears a phenyl substituent at C3, similarly to *cis*-**6**, and shows a different trend in the non-planarity of the *β*-lactam ring, denoting a higher conformational flexibility of the system. Conformers *cis*-**2a**, *cis*-**2b** and *cis*-**2c** show negative ψ_2 values, unlike other *cis* conformers, but show positive OR, which is consistent with the *β*-lactam sector rules. Conformer *cis*-**2g** shows a different orientation of the hydroxyl group (negative ω value) and a positive OR of lower magnitude. Finally, conformer *cis*-**2h** shows a negative ω value and a different orientation of the phenyl ring at C3 (ϕ_2 ~ 135°); this conformer shows a negative OR, in contrast to the *β*-lactam sector rules (Figure 6).

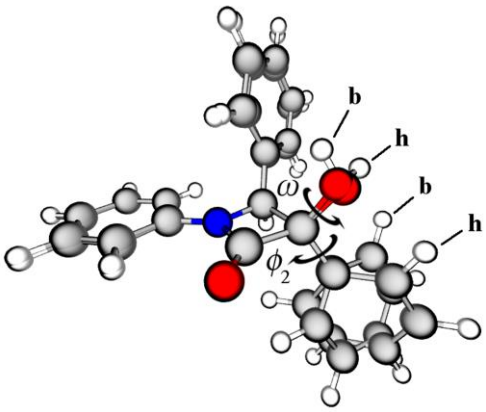

Figure 6. B97D/TZ2P optimised geometries of *cis*-**2h** and *cis*-**2b**. Solvation model: chloroform (IEFPCM). Dihedral angles are reported in Table 5.

Solvent-induced flexibility (SSM calculations)

Regular patterns are not observed for the SSM conformations (*cis*-**4*** and *cis*-**5***); the introduction of solvent molecules, interacting with the solute through hydrogen bonding, describes the molecular

geometry in solution in a more accurate fashion and induces a more complex pattern for the geometric features of the *β*-lactam ring, which is not possible to rationalise with semi-empirical rules. Another limiting factor is the presence of solvent molecules in TD-DFT calculations: the analysis of their direct and indirect contributions to the final values of theoretical $[\alpha]_D$ is beyond the aims of the present study and makes the correlation of chiroptical properties to the geometry of the solute very difficult.

*Conformational flexibility of cis-**6***

Interestingly, the same behaviour is observed for the geometry of the *β*-lactam ring of *cis*-**6**, even in the absence of explicit solvent molecules in the calculations: the conformational flexibility of the system is therefore much higher than for other derivatives. A deeper analysis, however, allows to identify the reasons behind the failure of the *β*-lactam sector rules in predicting the stereochemistry for this compound. Conformers having the thienyl substituent at C4 oriented with the sulphur atom towards the *β*-lactam ring (negative ϕ_1 values) all show negative OR values, which is consistent with the observations made on *cis*-**4** and *cis*-**5**. Among the conformers with opposite orientation of the heterocycle (positive ϕ_1 values, Figure 7), only *cis*-**6c** shows a negative torsion angle of the amide (ψ_1) and a positive $[\alpha]_D$ value, as expected by the helicity rule. Conformers *cis*-**6a** and *cis*-**6g** show a positive ψ_1 value and, similarly to what was observed for *cis*-**2h**, a different orientation of the phenyl ring at C3, thus showing negative OR. Finally, conformer *cis*-**6d** shows a different orientation of the hydroxyl group (negative ω value) and a negative $[\alpha]_D$ value of low magnitude, which is in accordance with the negative contribution to OR observed for *cis*-**2g**.

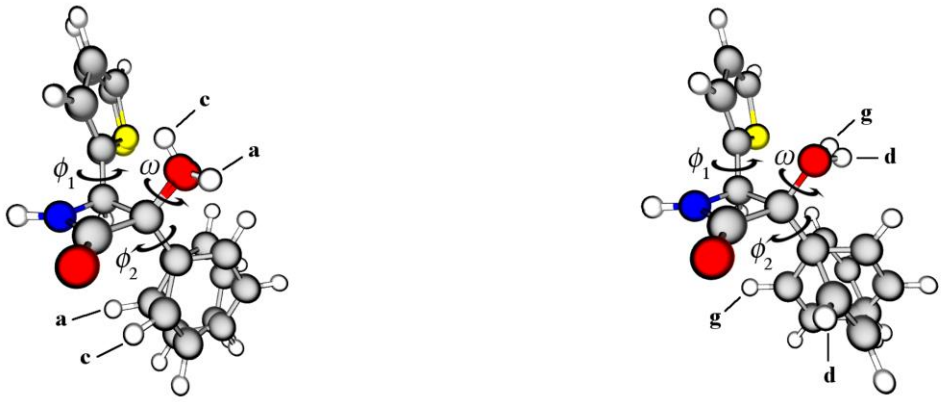

Figure 7. B97D/TZ2P optimised conformers of *cis*-**6** with positive values of ϕ_1. *Left*, *cis*-**6a** and *cis*-**6c**. *Right*, *cis*-**6d** and *cis*-**6g**. Solvation model: chloroform (IEFPCM). Dihedral angles are reported in Table 6.

Therefore, the presence of a phenyl substituent at C3 has a double effect: **a)** the regular trend in the geometric features of the β-lactam ring is perturbed and the conformational flexibility is increased, as observed for the optimised conformers of *cis*-**2** and *cis*-**6**; **b)** similarly to the orientation of heteroaromatic substituents, the orientation of the phenyl ring affects the chiroptical properties of these β-lactam derivatives to a great extent, resulting in a strong negative contribution to the calculated $[\alpha]_D$ values for some specific orientations (e.g., conformers *cis*-**2h**, *cis*-**6a** and *cis*-**6g**). Since these additional contributions are not considered in the definition of general chiroptical properties given by the semi-empirical β-lactam sector rules, the latter are unable to describe this behaviour appropriately and fail in the prediction of the correct relative configuration of *cis*-**6**.

CONCLUSIONS

TD-DFT calculations on a series of selected (3*R*)-3-hydroxy-4-aryl-*β*-lactam derivatives were successfully employed to confirm their absolute configuration and allowed to verify the validity of the semi-empirical *β*-lactam sector rules for the stereochemical characterisation of these compounds. The close relationship between the presence of regular patterns in the geometric parameters of *β*-lactam rings and the applicability of sector rules was identified, and the reasons behind their failure for the characterisation of a specific derivative, *cis*-**6**, were unveiled: the presence of a heterocyclic substituent at C4 and a phenyl substituent at C3 introduces additional complexity to the geometric and electronic features of this derivative, increasing its conformational flexibility and affecting its chiroptical properties.

Semi-empirical rules for the determination of the absolute configuration of chiral molecules are very useful tools, since the correlation between chiroptical properties and stereochemistry may be easily found by a fast and simple analysis of the position of substituents around a particular chromophore. However, these rules may fail when the nature of substituents affects the molecular geometry and electronic properties of the chromophore: this was the case for *cis*-**6**, where both the aromatic substituents at C3 and C4 induced large modifications to the general chiroptical properties predicted by the *β*-lactam sector rules.

First-principles methods, such as TD-DFT calculations, are very powerful tools for the determination of theoretical chiroptical properties, and their predictive power is becoming increasingly accurate and efficient as more complex theoretical models are being developed and the needed computational power is becoming available. Nevertheless, particular attention must be paid for the description of molecular geometry at equilibrium: a standard conformational analysis using implicit solvation may not reproduce faithfully the system when perturbations due to short-range interactions with the solvent become relevant. Higher levels of complexity, such as the SSM approach, should be considered in the calculations of chiroptical properties, especially in OR

calculations, whenever hydrogen bonding between solute and solvent may affect the chemical environment of the chromophore.

The present study highlighted the great importance of conformational flexibility for stereochemical characterisation: a detailed description of even small modifications in molecular geometry is fundamental for a reliable correlation between experimental chiroptical properties and chemical structure of chiral molecules in solution.

ACKNOWLEGDEMENTS

The authors are grateful for financial support from the University of Bologna and from MIUR, Italy (PRIN 2008 National Program).

REFERENCES

[1] Lukacs G, Ohno M, editors. Recent progress in the chemical synthesis of antibiotics. Berlin: Springer-Verlag; 1990.

[2] Morin RB, Gorman M, editors. Chemistry and biology of β-lactam antibiotics, vol. 1-3. New York: Academic Press; 1982.

[3] Sammes PG, editor. Topics in antibiotic chemistry, vol. 3. New York: Ellis Horwood; 1980.

[4] O'Sullivan J, Abraham EP. Biosynthesis of β-lactam antibiotics. In: Corcoran JW, editor. Antibiotics, vol. IV, Biosynthesis. Berlin: Springer-Verlag; 1982. pp. 101–122.

[5] Bentley PM, Southgate R, editors. Recent advances in the chemistry of β-lactam antibiotics. London: The Royal Society of Chemistry; 1989.

[6] Christensen BG. Structure-activity relationships in β-lactam antibiotics. In: Salton MRJ, Shockman GD, editors. β-Lactam antibiotics. New York: Academic Press; 1981. pp. 101–122.

[7] Burnett DA, Caplen MA, Davis HR, Burrier RE, Clader JW. 2-azetidinones as inhibitors of cholesterol absorption. J Med Chem 1994;37:1733–1736.

[8] Braun M, Galle D. A simple stereoselective synthesis of the cholesterol absorption inhibitor (−)-SCH 48461. Synthesis 1996;1996:819–820.

[9] Chen LY, Zaks A, Chackalamannil S, Dugar S. Asymmetric synthesis of substituted 2-azaspiro[3.5]nonan-1-ones: an enantioselective synthesis of the cholesterol absorption inhibitor (+)-SCH 54016. J Org Chem 1996;61:8341–8343.

[10] Adlington RM, Baldwin JE, Becker GW, Chen B, Cheng L, Cooper SL, Hermann RB, Howe TJ, McCoull W, McNulty AM, Neubauer BL, Pritchard GJ. Design, synthesis, and proposed active site binding analysis of monocyclic 2-azetidinone inhibitors of prostate specific antigen. J Med Chem 2001;44:1491–1508.

[11] Ojima I. β-Lactam synthon method - Enantiomerically pure β-lactams as synthetic intermediates. In: Georg GI, editor. The organic chemistry of β-lactam antibiotics. New York: VCH; 1992a. pp. 197–255.

[12] Ojima I, Habus I, Zhao M, Zucco M, Park YH, Sun CM, Brigaud T. New and efficient approaches to the semisynthesis of taxol and its C-13 side chain analogs by means of β-lactam synthon method. Tetrahedron 1992b;48:6985–7012.

[13] Ojima I. Recent advances in the β-lactam synthon method. Acc Chem Res 1995;28:383–389.

[14] Ojima I, Delaloge F. Asymmetric synthesis of building-blocks for peptides and peptidomimetics by means of the β-lactam synthon method. Chem Soc Rev 1997;26:377–386.

[15] Palomo C, Aizpurua JM, Ganboa I, Oiarbide M. β-Lactams as versatile intermediates in α- and β-amino acid synthesis. Synlett 2001;2001:1813–1826.

[16] Barbaro G, Battaglia A, Guerrini A, Bertucci C. One-pot synthesis of (3R)-hydroxy-β-lactams via enolates of 2-tert-butyl-1,3-dioxolan-4-ones. Part 1. Tetrahedron: Asymmetry 1997;8:2527–2531.

[17] Barbaro G, Battaglia A, Guerrini A, Bertucci C. (3R)-Chiral control of 3-alkyl-3-hydroxy-β-lactams via addition reaction of imines to enolates of 1,3-dioxolan-4-ones. J Org Chem 1999a;64:4643–4651.

[18] Barbaro G, Battaglia A, Di Giuseppe F, Giorgianni P, Guerrini A, Bertucci C, Geremia S. New efficient synthesis of (3R,4S)-3-methyl-3-hydroxy-4-phenyl-β-lactam. Tetrahed Asym 1999b;10:2765–2773.

[19] Battaglia A, Guerrini A, Bertucci C. Synthesis of optically active constrained 2-substituted norstatines: a straightforward application of Seebach's "SRS" synthetic principle. J Org Chem 2004;69:9055–9062.

[20] Seebach D, Sting AR, Hoffmann M. Self-regeneration of stereocenters (SRS) - Applications, limitations, and abandonment of a synthetic principle. Angew Chem Int Ed Engl 1996;35:2708–2748.

[21] Rehling H, Jensen H. Circulardichroismus und absolute Konfiguration von β-Lactamen. Tetrahed Lett 1972;13:2793–2796.

[22] Ong EC, Cusachs LC, Weigang Jr OE. Sector rules for rotatory strength of low symmetry chromophores: lactones, lactams, and peptides. J Chem Phys 1977;67:3289–3297.

[23] Polonski T, Milewska MJ. Optical activity of lactones and lactams. 5. Long-wavelength circular dichroism of β-thiolactams (2-azetidinethiones). Croat Chim Acta 1989;62:129–134.

[24] Galle D, Tolksdorf M, Braun M. Circular dichroism of trans and cis β-lactams and of their inclusion compounds in β-cyclodextrin. Tetrahed Lett 1995;36:4217–4220.

[25] Djerassi C. Optical rotatory dispersion: applications to organic chemistry. New York: McGraw-Hill; 1960.

[26] Moffitt W, Woodward RB, Moscowitz A, Klyne W, Djerassi C. Structure and the optical rotatory dispersion of saturated ketones. J Am Chem Soc 1961;83:4013–4018.

[27] Lightner DA. The octant rule. In: Berova N, Nakanishi K, Woody R, editors. Circular dichroism: principles and applications, 2nd edition. New York: Wiley-VCH; 2000. pp. 261–303.

[28] Boyd D, Riehl J, Richardson F. Chiroptical properties of 1-carbapenam and orbital mixing in

nonplanar amides. Tetrahedron 1979;35:1499–1508.

[29] McCann J, Rauk A, Shustov GV, Wieser H, Yang D. Electronic and vibrational circular dichroism of model β-lactams: 3-methyl- and 4-methylazetidin-2-one. Appl Spectr 1996;50:630–641.

[30] Łysek R, Borsuk K, Chmielewski M, Kałuża Z, Urbańczyk-Lipkowska Z, Klimek A, Frelek J. 5-Dethia-5-oxacephams: toward correlation of absolute configuration and chiroptical properties. J Org Chem 2002;67:1472–1479.

[31] Frelek J, Kowalska P, Masnyk M, Kazimierski A, Korda A, Woźnica M, Chmielewski M, Furche F. Circular dichroism and conformational dynamics of cephams and their carba and oxa analogues. Chem Eur J 2007;6732–6744.

[32] Huang X, Rickman BH, Borhan B, Berova N, Nakanishi K. Zinc porphyrin tweezer in host-guest complexation: determination of absolute configurations of diamines, amino acids, and amino alcohols by circular dichroism. J Am Chem Soc 1998;120:6185–6186.

[33] Berova N, Nakanishi K. Exciton chirality method: principles and applications. In: Berova N, Nakanishi K, Woody R, editors. Circular dichroism: principles and applications, 2nd edition. New York: Wiley-VCH; 2000. pp. 337–382.

[34] Petrovic AG, Chen Y, Pescitelli G, Berova N, Proni G. CD-sensitive Zn-porphyrin tweezer host-guest complexes, part 1: MC/OPLS-2005 computational approach for predicting preferred interporphyrin helicity. Chirality 2010;22:129–139.

[35] Chen Y, Petrovic AG, Roje M, Pescitelli G, Kayser MM, Yang Y, Berova N, Proni G. CD-sensitive Zn-porphyrin tweezer host-guest complexes, part 2: Cis- and trans-3-hydroxy-4-aryl/alkyl-β-lactams. A case study. Chirality 2010;22:140–152.

[36] Barbaro G, Battaglia A, Guerrini A, Bertucci C. Assessment of the absolute configuration of a series of (3R)-3-hydroxy-3-alkyl-β-lactams. Tetrahedron: Asymmetry 1998;9:3401–3409.

[37] Bauernschmitt R, Ahlrichs R. Treatment of electronic excitations within the adiabatic approximation of time dependent density functional theory. Chem Phys Lett 1996;256:454–464.

[38] Hohenberg P, Kohn W. Inhomogenous electron gas. Phys Rev 1964;136:B864–B871.

[39] Kohn W, Sham LJ. Self-consistent equations including exchange and correlation effects. Phys Rev 1965;140:A1133–A1138.

[40] Spartan’02. Wavefunction, Inc., Irvine, CA, USA.

[41] Halgren TA. MMFF VI. MMFF94s option for energy minimization studies. J Comput Chem 1999;20:720–729.

[42] Becke AD. Density-functional thermochemistry. V. Systematic optimization of exchange-correlation functionals. J Chem Phys 1997;107:8554–8560.

[43] Grimme S. Semiempirical GGA-type density functional constructed with a long-range dispersion correction. J Comput Chem 2006;27:1787–1799.

[44] Gaussian 09, Revision A.02. Frisch MJ, Trucks GW, Schlegel HB, Scuseria GE, Robb MA, Cheeseman JR, Scalmani G, Barone V, Mennucci B, Petersson GA, Nakatsuji H, Caricato M, Li X, Hratchian HP, Izmaylov AF, Bloino J, Zheng G, Sonnenberg JL, Hada M, Ehara M, Toyota K, Fukuda R, Hasegawa J, Ishida M, Nakajima T, Honda Y, Kitao O, Nakai H, Vreven T, Montgomery Jr JA, Peralta JE, Ogliaro F, Bearpark M, Heyd JJ, Brothers E, Kudin KN, Staroverov VN, Kobayashi R, Normand J, Raghavachari K, Rendell A, Burant JC, Iyengar SS, Tomasi J, Cossi M, Rega N, Millam JM, Klene M, Knox JE, Cross JB, Bakken V, Adamo C, Jaramillo J, Gomperts R, Stratmann RE, Yazyev O, Austin AJ, Cammi R, Pomelli C, Ochterski JW, Martin RL, Morokuma K, Zakrzewski VG, Voth GA, Salvador P, Dannenberg JJ, Dapprich S, Daniels AD, Farkas Ö, Foresman JB, Ortiz JV, Cioslowski J, Fox DJ. Gaussian, Inc., Wallingford, CT, 2009.

[45] Dunning TH. Gaussian basis functions for use in molecular calculations. III. Contraction of (10s6p) atomic basis sets for the first-row atoms. J Chem Phys 1971;55:716–723.

[46] Huzinaga S. Gaussian-type functions for polyatomic systems. I. J Chem Phys 1965;42:1293–1302.

[47] McLean AD, Chandler GS. Contracted Gaussian basis sets for molecular calculations. I. Second row atoms, Z=11-18. J Chem Phys 1980;72:5639–5648.

[48] Huzinaga S. Approximate atomic functions. II. Department of Chemistry, University of Alberta, Edmonton; 1971.

[49] Tomasi J, Mennucci B, Cammi R. Quantum mechanical continuum solvation models. Chem Rev 2005;105:2999–3094.

[50] Humphrey W, Dalke A, Schulten K. VMD: visual molecular dynamics. J Mol Graphics 1996;14:33–38.

[51] Ditchfield R, Hehre WJ, Pople JA. Self-consistent molecular orbital methods. IX. An extended Gaussian-type basis for molecular orbital studies of organic molecules. J Chem Phys 1971;54:724–728.

[52] Hehre WJ, Ditchfield R, Pople JA. Self-consistent molecular orbital methods. XII. Further extensions of Gaussian-type basis sets for use in molecular orbital studies of organic molecules. J Chem Phys 1972;56:2257–2261.

[53] Hariharan PC, Pople JA. The influence of polarization functions on molecular orbital hydrogenation energies. Theor Chem Acc 1973;28:213–222.

[54] Gordon MS. The isomers of silacyclopropane. Chem Phys Lett 1980;76:163–168.

[55] Frisch MJ, Pople JA, Binkley JS. Self-consistent molecular orbital methods. XXV. Supplementary functions for Gaussian basis sets. J Chem Phys 1984;80:3265–3269.

[56] Autschbach J. Computing chiroptical properties with first-principles theoretical methods: background and illustrative examples. Chirality 2009;21:E116–E152.

[57] Perdew JP, Burke K, Ernzerhof M. Generalized gradient approximation made simple. Phys Rev Lett 1996;77:3865–3868.

[58] Perdew JP, Burke K, Ernzerhof M. Generalized gradient approximation made simple [Phys. Rev. Lett. 77, 3865 (1996)]. Phys Rev Lett 1997;78:1396–1396.

[59] Adamo C, Barone V. Toward reliable density functional methods without adjustable parameters: the PBE0 model. J Chem Phys 1999;110:6158–6170.

[60] Stephens PJ, Harada N. ECD Cotton effect approximated by the Gaussian curve and other methods. Chirality 2010;22:229–233.

[61] Taylor JR. Introduction to error analysis: the study of uncertainties in physical measurements, 2nd edition. Sausalito: University Science Books; 1997.

[62] Pescitelli G, Di Bari L, Berova N. Conformational aspects in the studies of organic compounds by electronic circular dichroism. Chem Soc Rev 2011;40:4603–4625.